Supplement of Atmos. Meas. Tech., 18, 1961–1979, 2025
https://doi.org/10.5194/amt-18-1961-2025-supplement

Atmospheric Measurement Techniques
Open Access

Supplement of

Improved consistency in solar-induced fluorescence retrievals from GOME-2A with the SIFTER v3 algorithm

Juliëtte C. S. Anema et al.

Correspondence to: Juliëtte C. S. Anema (juliette.anema@knmi.nl)

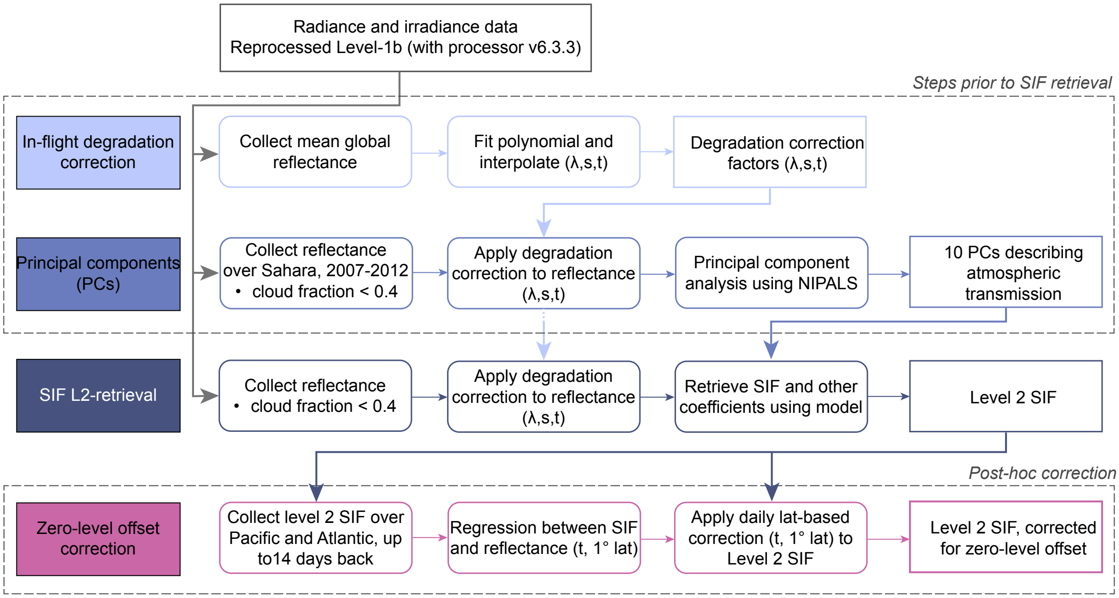

Figure S1. Flowchart showing the basic steps to retrieve Level-2 SIF from GOME-2A using the SIFTER v3 algorithm.

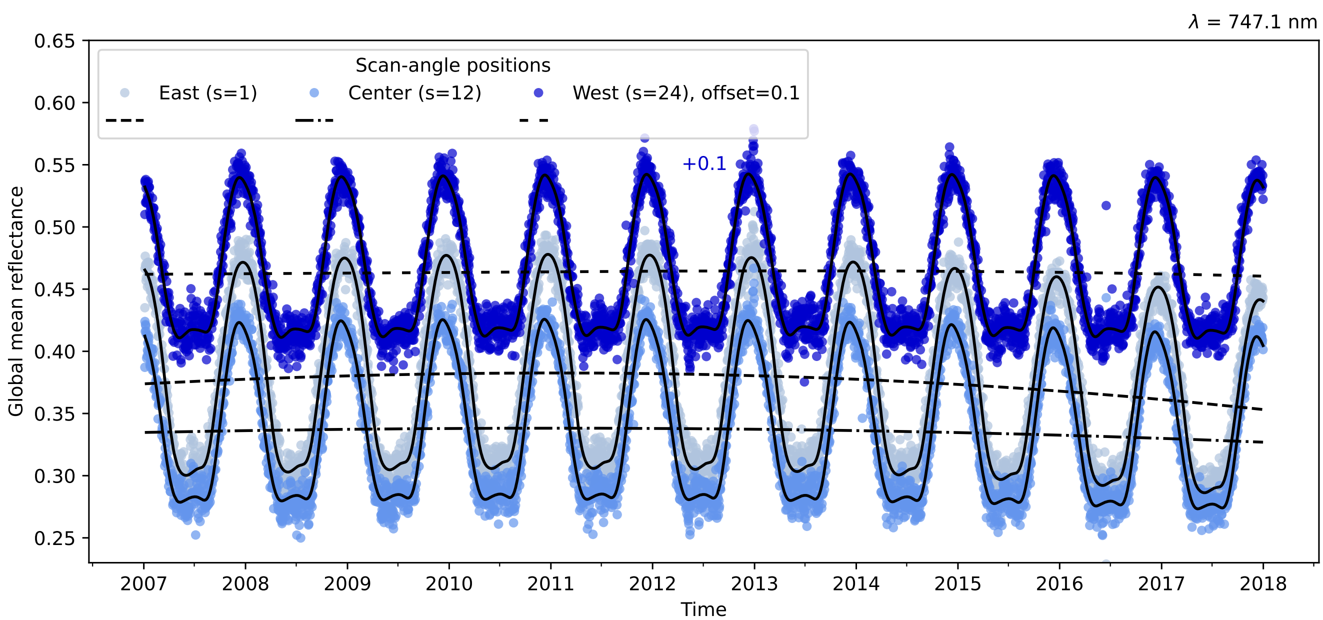

Figure S2. Global mean daily reflectance at 747.1 nm from GOME-2A over time, between 2007 and 2017, for the most eastward (s=0), center (s=12), and most westward (s=24) scan angle positions. See also the caption of Fig. 2 from the manuscript.

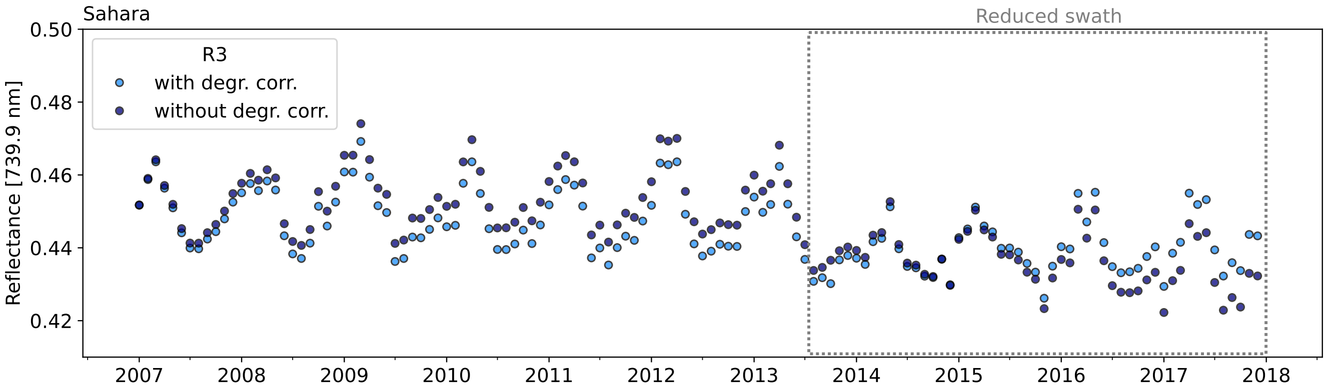

Figure S3. Time series of monthly averaged level-1b Release 3 (R3) reflectance data at 739.9 nm over the Sahara including (denoted in blue) and excluding (denoted in navy) the in-flight degradation correction. The reduced swath period is indicated by the dashed box.

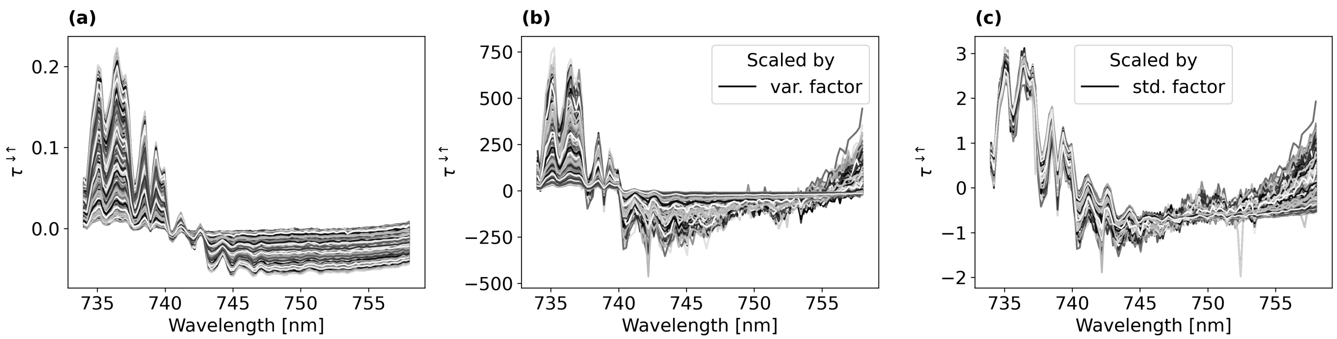

Figure S4. (a) Centralized two-way slant absorption optical thickness $\tau^{\uparrow\downarrow}$ spectra over the Sahara reference area between 2007 and 2012. Panels (b) and (c) show the centralized and scaled spectra, scaled by the variance and standard deviation factor, respectively.

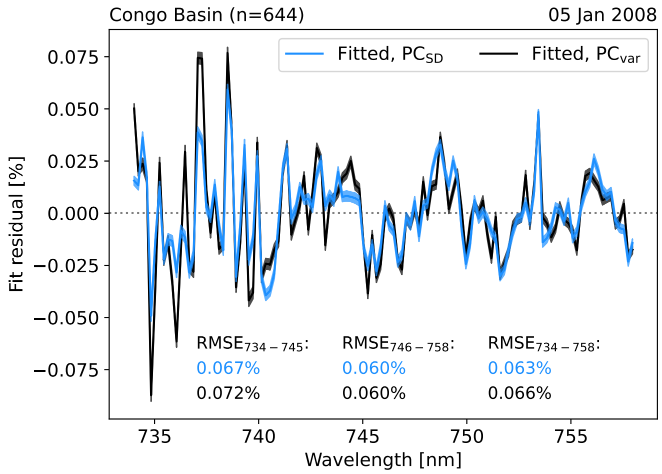

Figure S5. Average fit residuals of 644 pixels over the Congo Basin at 5 January 2008 obtained with PCs that used standard deviation scaling (denoted in blue) and PCs that used variance scaling (denoted in black). All other settings follow that of SIFTER v3.

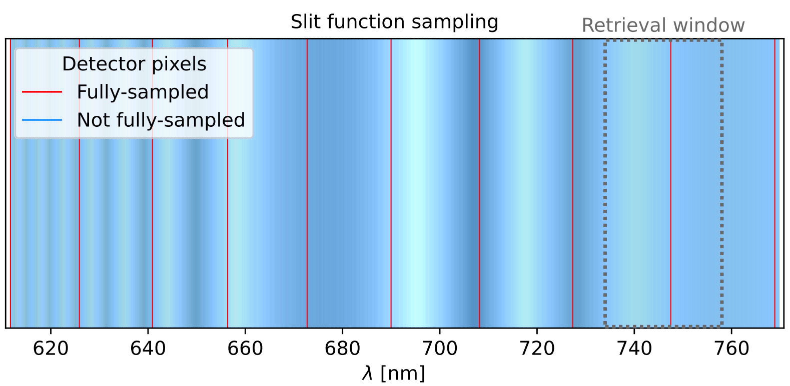

Figure S6. Location of all fully and not-fully sampled pixels that contain slit function information. The SIF retrieval window is indicated by the grey dashed line.

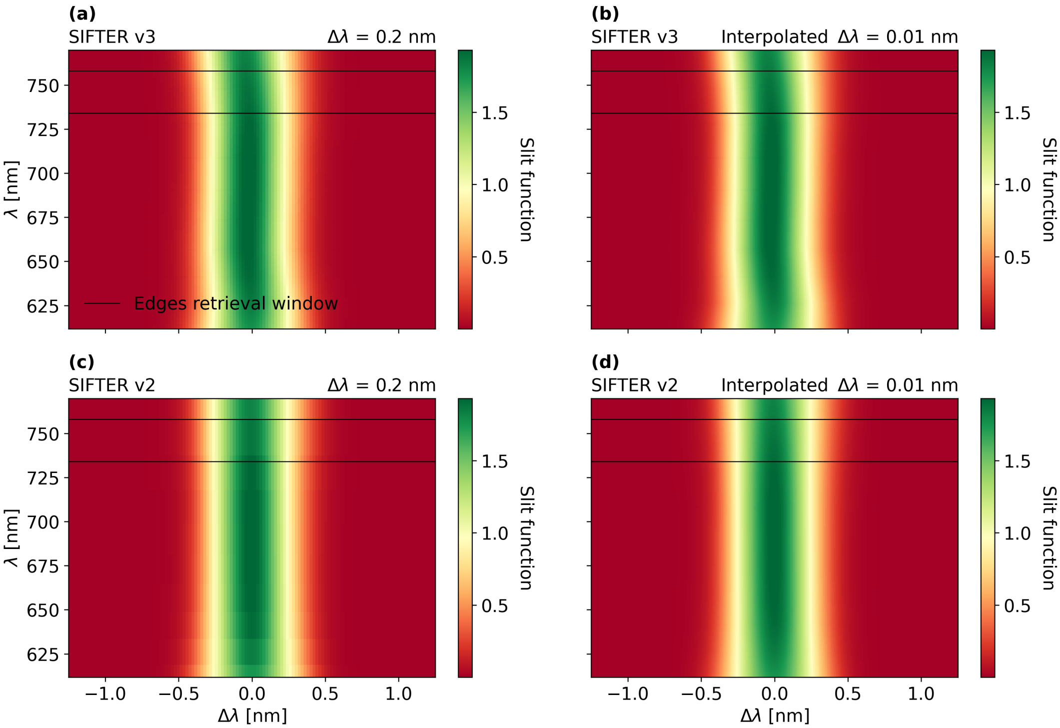

Figure S7. Slit functions of all (a) fully and not-fully sampled detector pixels (n=765), as done in SIFTER v3, and (c) only fully sampled detector pixels (n=10), as done in SIFTER v2, with the spectral resolution of 0.2 nm. The two right panels show the results of the interpolation across the slit functions to the spectral resolution of Chance and Kurucz at 0.01 nm, using (b) all pixels as input and (d) only the fully-sampled pixels as input.

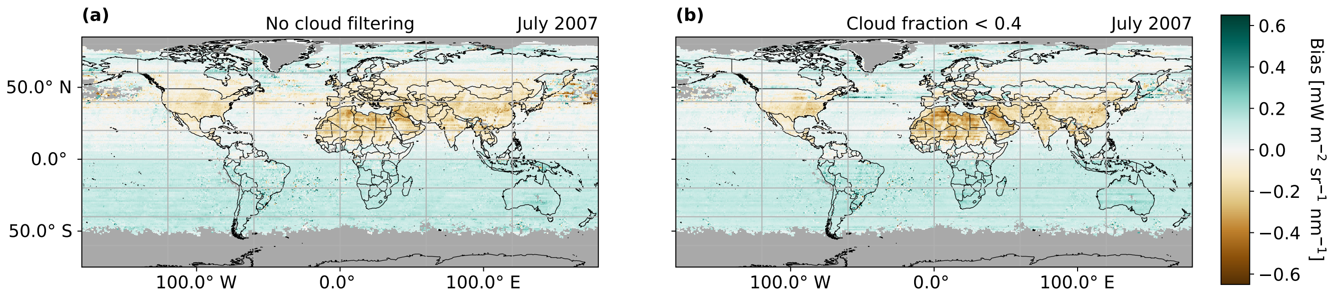

Figure S8. Gridded zero-level adjustment biases ($0.5^\circ \times 0.5^\circ$) over July 2007 of SIFTER v3 (a) without cloud filtering and (b) with pixels that met the criteria of cloud fractions <0.4 (as done in SIFTER v2).

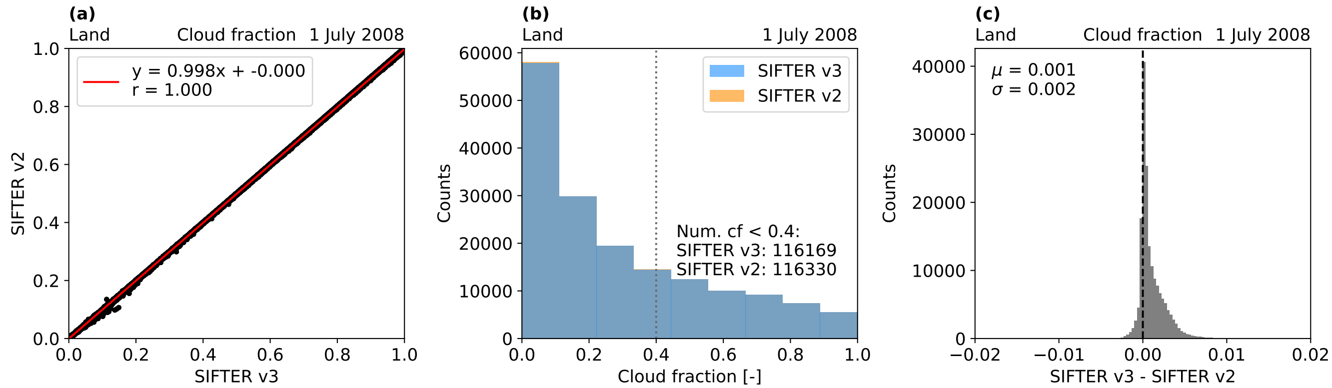

Figure S9. Difference in cloud fractions of SIFTER v3 and SIFTER 2, due to different versions of FRESCO+. Pixel-by-pixel comparisons of the (a) comparison of the cloud fractions in both products, (b) the histograms of both products and indicating the number of pixels that meet the criteria of <0.4, and (c) the difference between the cloud fraction in SIFTER v3 and SIFTER v2. All shown data represents land pixels at 1 July 2008.

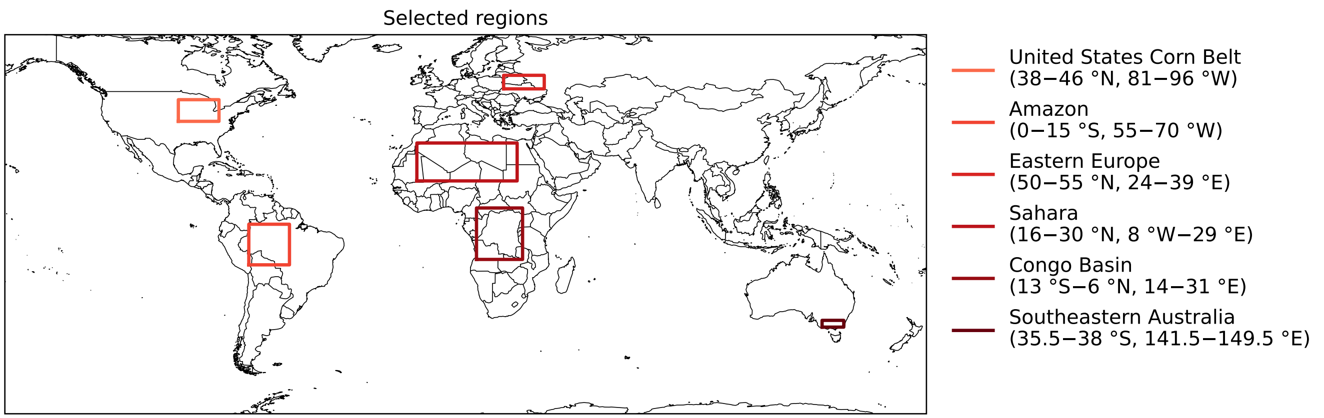

Figure S10. Locations of the selected regions in this study.

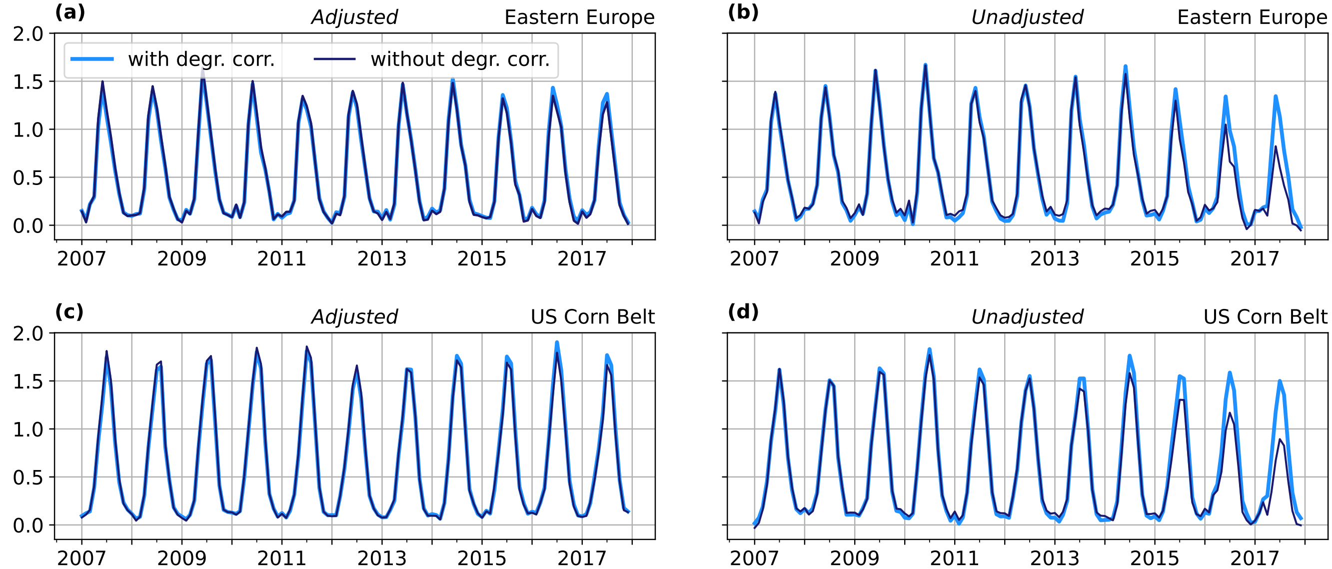

Figure S11. Time series of monthly averaged instantaneous SIFTER v3 values over eastern Europe (a,b) and the US Corn Belt (c,d), with (denoted in light blue) and without (denoted in dark blue) applied degradation correction. The left panels (a,c) show the values for the final product, including the zero-level adjustment, the right panels (b,d) show the values for the retrieved SIF without the zero-level adjustment.

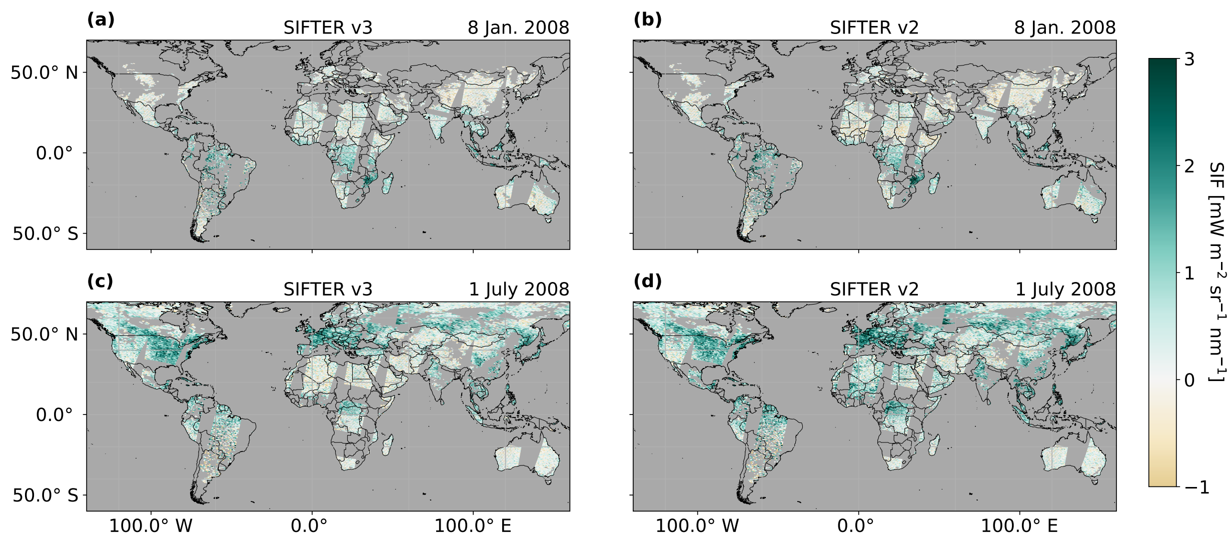

Figure S12. Daily instantaneous GOME-2A SIF values ($0.5^\circ \times 0.5^\circ$) from SIFTER v3 (a,c) and SIFTER v2 (b,d) at January 8th and the 1st of July 2008. SIFTER data was selected for autocorrelation values <0.2 and cloud fraction <0.4.

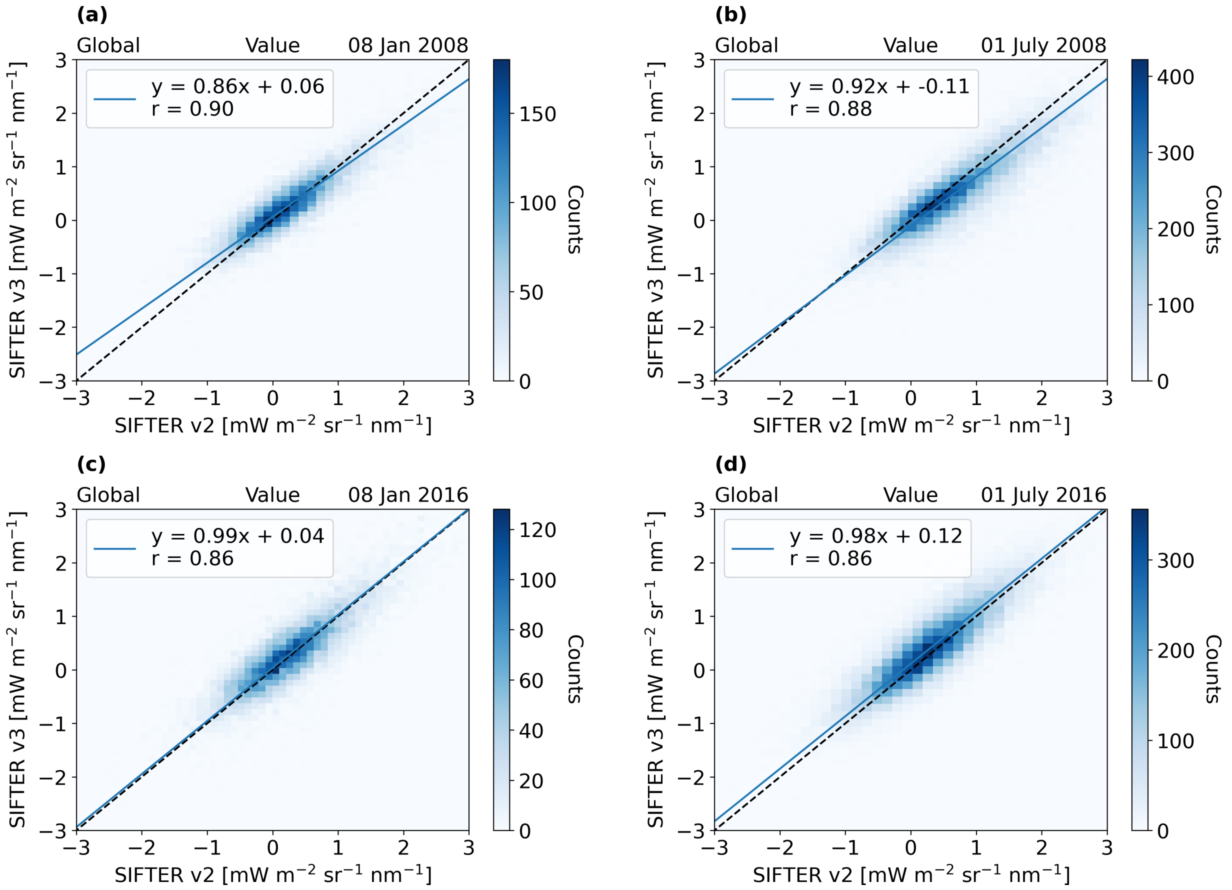

Figure S13. Pixel-by-pixel comparison of the instantaneous SIF values of SIFTER v3 and SIFTER v2 over all land-pixels on (a) 8 Jan 2008, (b) 1 July 2008, (c) 8 Jan. 2016, and (d) 1 July 2016. The pixels cover the global land area and are filtered for autocorrelation values <0.2 and cloud fractions <0.4.

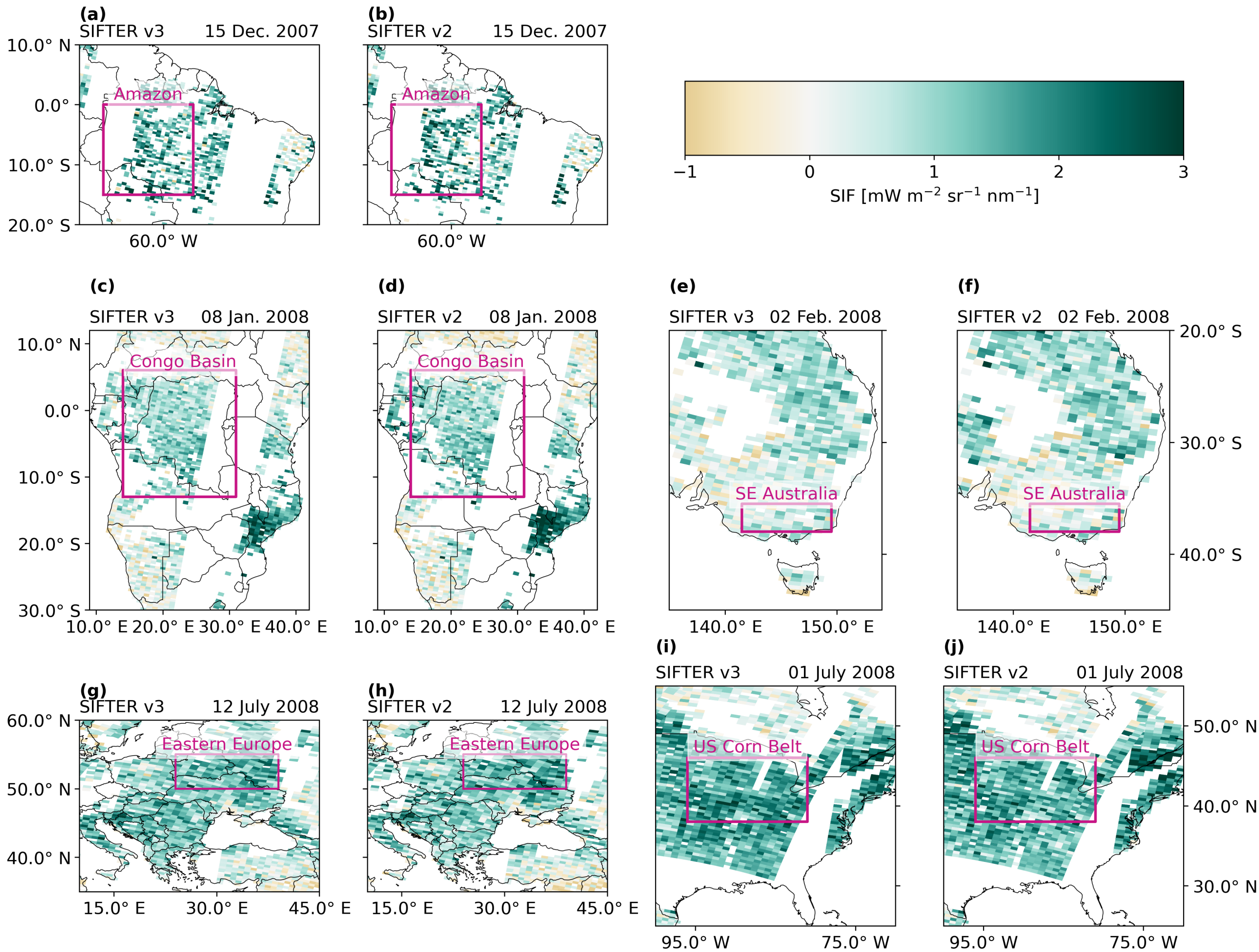

Figure S14. Maps across five vegetative showing the spatial variability of daily instantaneous SIF retrieved using the SIFTER v3 and SIFTER v2 algorithms. Days are selected to be within the peak season of the region, June–August for the Northern Hemisphere and December–January for the Southern Hemisphere. Regions shown are: (a,b) Amazon, (c,d) Congo Basin, (e,f) Southeastern Australia, (g,h) Eastern Europe, and (i,j) the United States Corn Beltt. Regions correspond to the areas shown in Fig. S10.

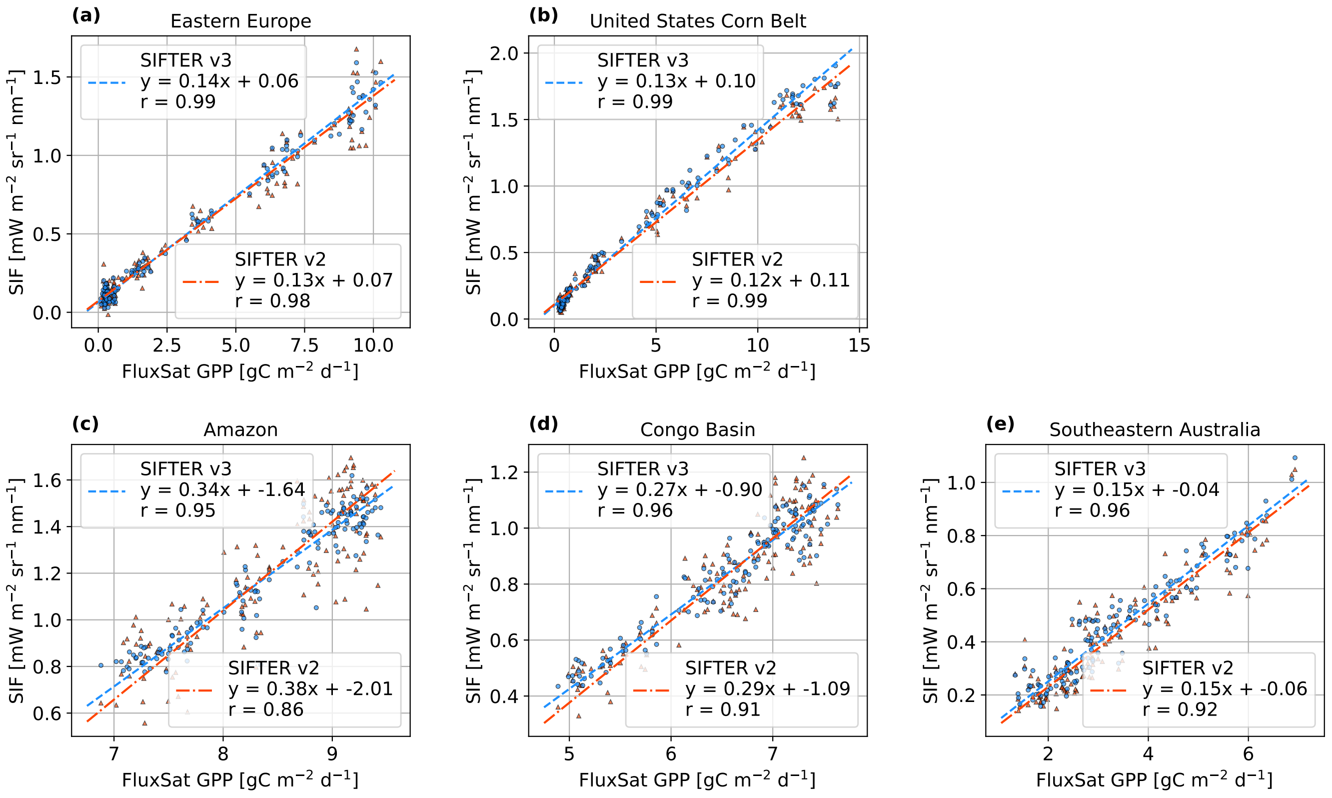

Figure S15. Comparison of monthly averaged FluxSat GPP with instantaneous SIF data from SIFTER v3 (blue bullets) and SIFTER v2 (orange triangles) across (a) eastern Europe, (b) United States Corn Belt, (c) the Amazon, (d) the Congo Basin, and (e) southeastern Australia.

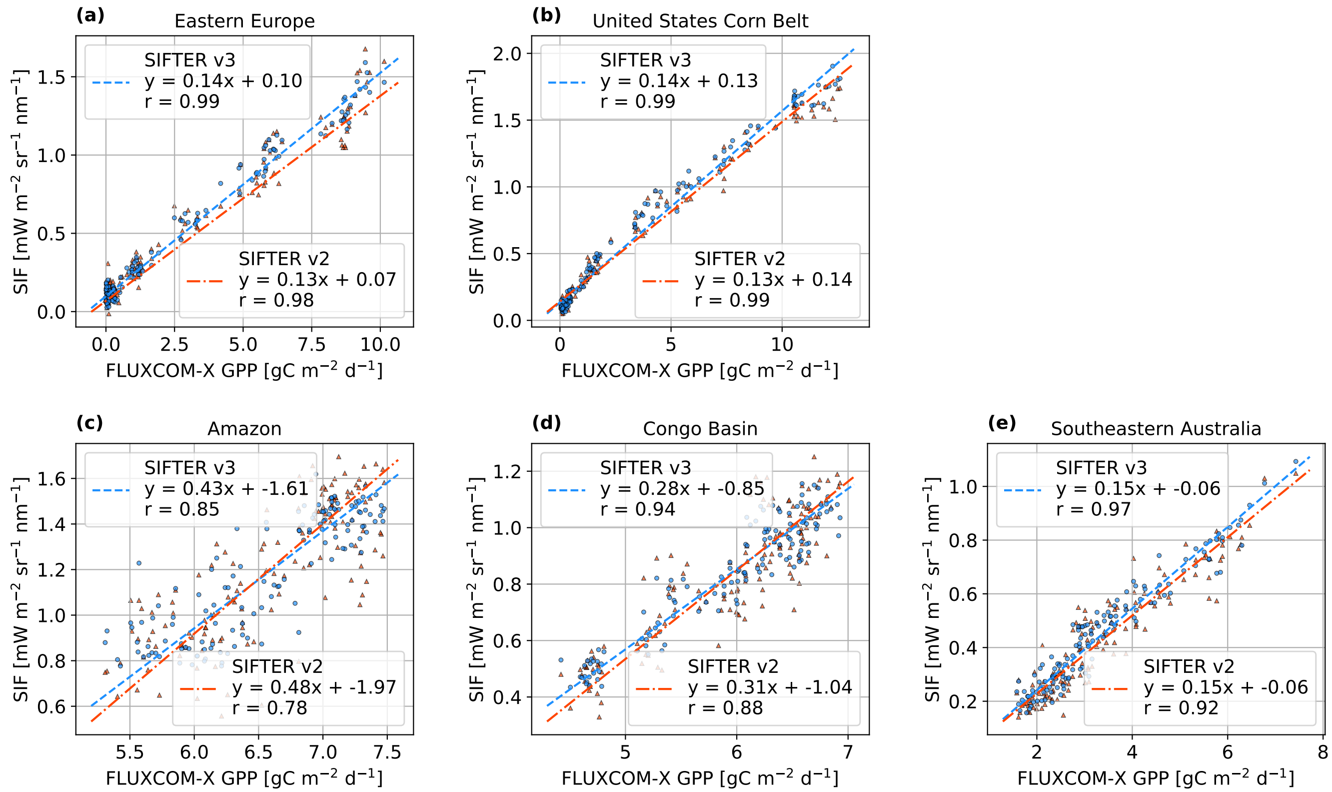

Figure S16. Comparison of monthly averaged FLUXCOM-X GPP with instantaneous SIF data from SIFTER v3 (blue bullets) and SIFTER v2 (orange triangles) across (a) eastern Europe, (b) United States Corn Belt, (c) the Amazon, (d) the Congo Basin, and (e) southeastern Australia.

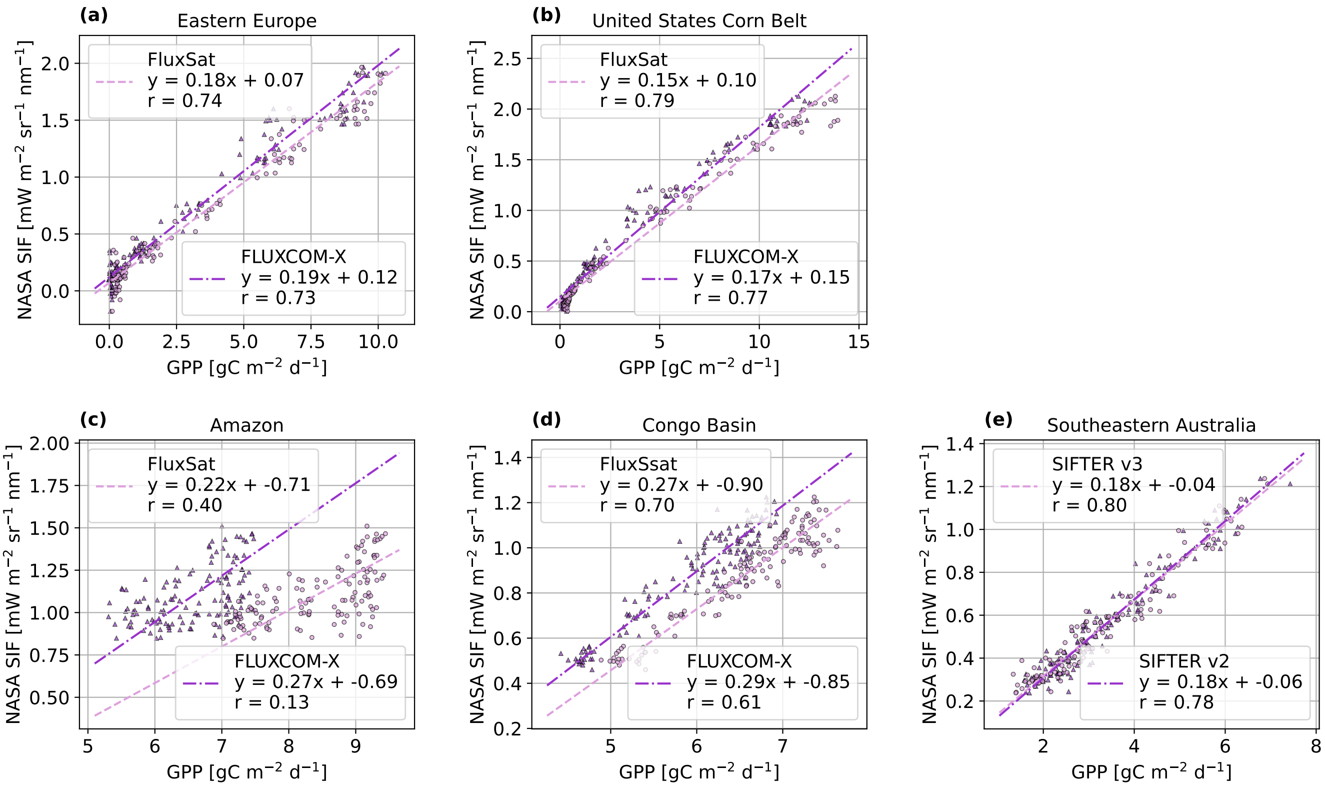

Figure S17. Comparison of monthly averaged FluxSat GPP (light purple bullets) and FLUXCOM-X GPP (dark purple triangles) with instantaneous SIF data from NASA GOME-2A SIF across (a) eastern Europe, (b) United States Corn Belt, (c) the Amazon, (d) the Congo Basin, and (e) southeastern Australia.

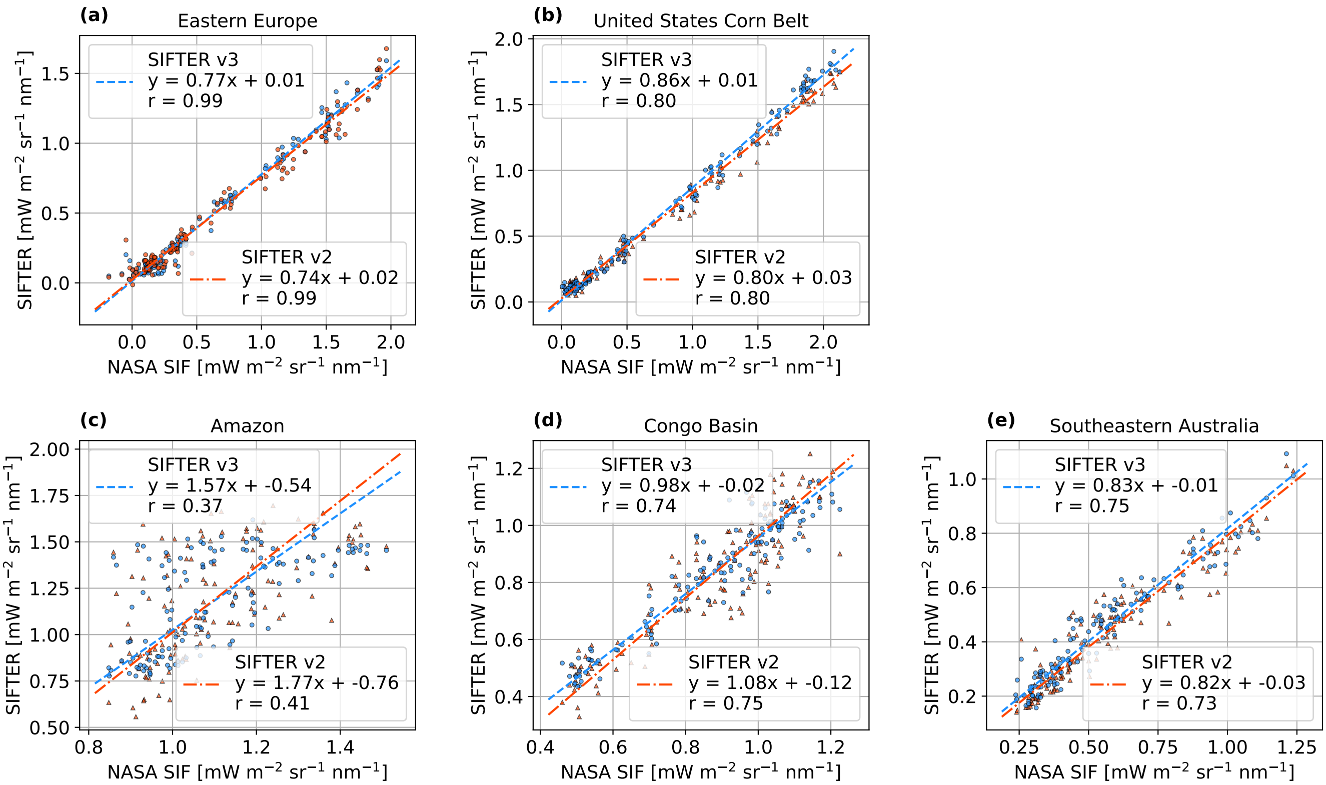

Figure S18. Comparison of monthly averaged instantaneous NASA GOME-2A SIF data with SIF data from SIFTER v3 (blue bullets) and SIFTER v2 (orange triangles) SIF across (a) eastern Europe, (b) United States Corn Belt, (c) the Amazon, (d) the Congo Basin, and (e) southeastern Australia.

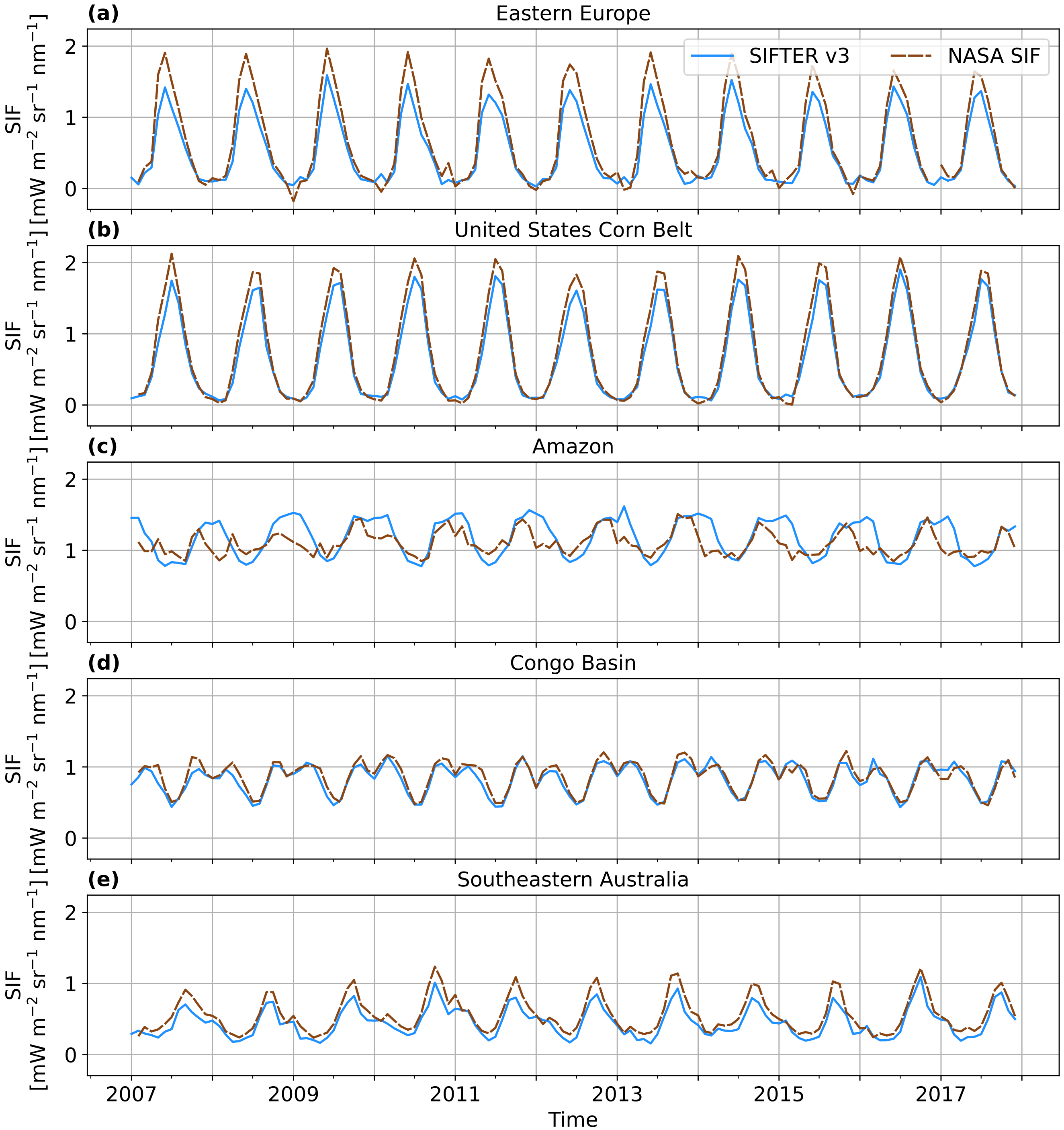

Figure S19. Time series of instantaneous SIFTER v3 (blue line) and NASA SIF (brown dashed line) across the five vegetative regions of Fig. S10.

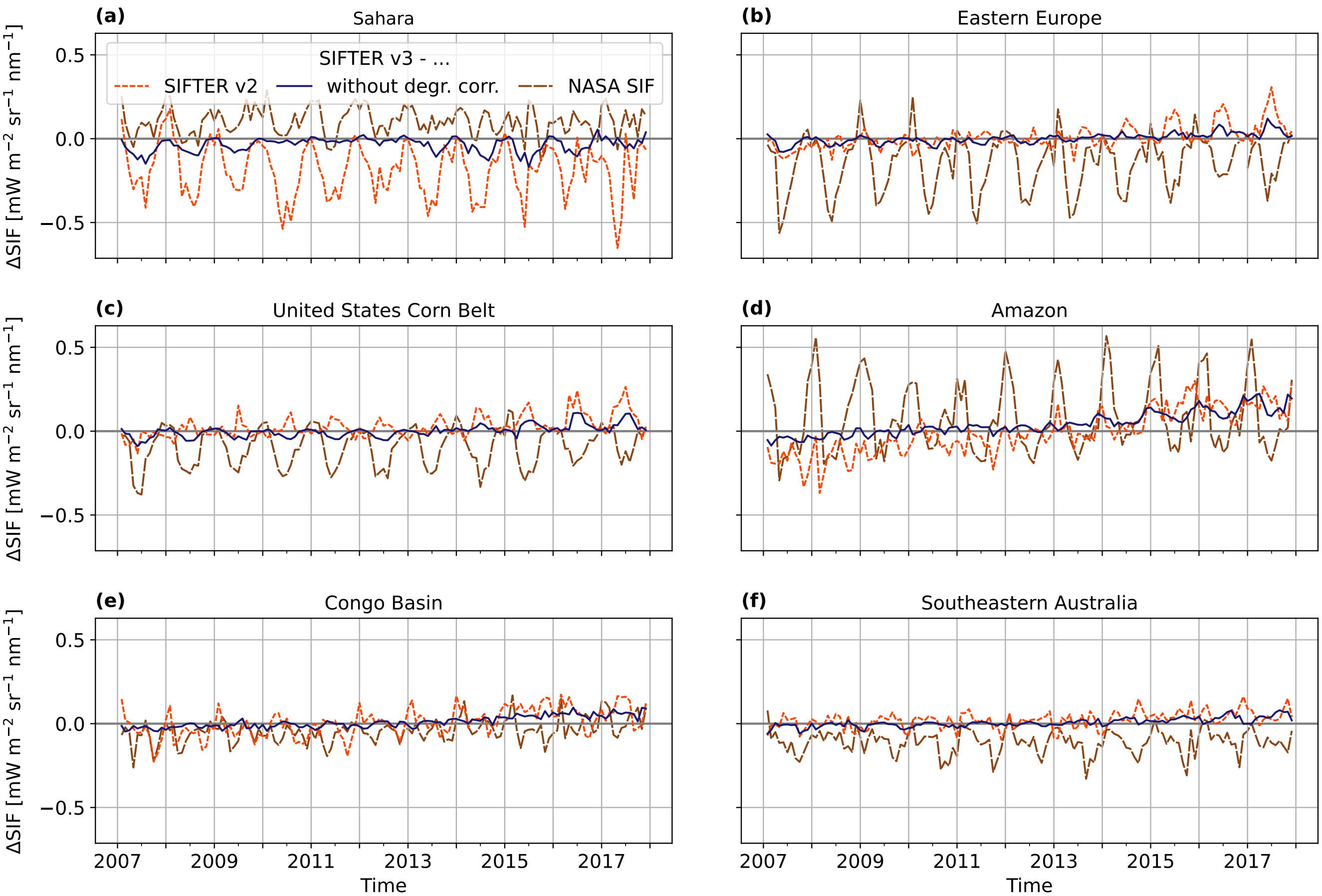

Figure S20. Time series of the difference between SIFTER v3 and SIFTER v2 (orange dashed line), SIFTER v3 without degradation correction (navy blue line), and NASA SIF (browned dashed line) across all six regions of Fig. S10. Value above 1 indicate higher values of SIFTER v3. All SIF data shown reflects instantaneous values.